Research Article | Vol. 26, No. 3 | 5 Feb 2018 | OPTICS EXPRESS 3067
Optics EXPRESS

Enhancement of high-order harmonics in a plasma waveguide formed in clustered Ar gas

XIAOTAO GENG,[1,2] SHIYANG ZHONG,[3] GUANGLONG CHEN,[4] WEIJUN LING,[5] XINKUI HE,[3] ZHIYI WEI,[3,6] AND DONG EON KIM[1,2,*]

[1]*Department of Physics, Center for Attosecond Science and Technology, Pohang University of Science and Technology, Pohang, Gyeongbuk 37673, Republic of Korea*
[2]*Max Planck POSTECH/KOREA Research Initiative, Pohang, Gyeongbuk 37673, Republic of Korea*
[3]*Beijing National Laboratory for Condensed Matter Physics, Institute of Physics, Chinese Academy of Sciences, Beijing, China*
[4]*School of Mathematics, Physics and Statistics, Shanghai University of Engineering Science, Shanghai 201620, China*
[5]*Department of physics, Tianshui Normal University, Tianshui, 741001, China*
[6]*School of Physical Science, University of Chinese Academy of Sciences, Beijing 100049, China*
[*]*kimd@postech.ac.kr*

Abstract: Generation of high-order harmonics (HHs) is intensified by using a plasma waveguide created by a laser in a clustered gas jet. The formation of a plasma waveguide and the guiding of a laser beam are also demonstrated. Compared to the case without a waveguide, harmonics were strengthened up to nine times, and blue-shifted. Numerical simulation by solving the time-dependent Schrödinger equation in strong field approximation agreed well with experimental results. This result reveals that the strengthening is the result of improved phase matching and that the blue shift is a result of change in fundamental laser frequency due to self-phase modulation (SPM).

OCIS codes: (190.2620) Harmonic generation and mixing; (270.6620) Strong-field processes; (320.7110) Ultrafast nonlinear optics.

References and links

1. J. Itatani, J. Levesque, D. Zeidler, H. Niikura, H. Pépin, J. C. Kieffer, P. B. Corkum, and D. M. Villeneuve, "Tomographic imaging of molecular orbitals," Nature **432**(7019), 867–871 (2004).
2. S. Baker, J. S. Robinson, C. A. Haworth, H. Teng, R. A. Smith, C. C. Chirilă, M. Lein, J. W. G. Tisch, and J. P. Marangos, "Probing proton dynamics in molecules on an attosecond time scale," Science **312**(5772), 424–427 (2006).
3. Z. H. Loh, M. Khalil, R. E. Correa, R. Santra, C. Buth, and S. R. Leone, "Quantum state-resolved probing of strong-field-ionized xenon atoms using femtosecond high-order harmonic transient absorption spectroscopy," Phys. Rev. Lett. **98**(14), 143601 (2007).
4. M. E. Siemens, Q. Li, R. Yang, K. A. Nelson, E. H. Anderson, M. M. Murnane, and H. C. Kapteyn, "Quasi-ballistic thermal transport from nanoscale interfaces observed using ultrafast coherent soft X-ray beams," Nat. Mater. **9**(1), 26–30 (2010).
5. S. C. Rae, "Ionization-induced defocusing of intense laser pulses in high-pressure gases," Opt. Commun. **97**(1-2), 25–28 (1993).
6. C. Altucci, T. Starczewski, E. Mevel, C. G. Wahlström, B. Carré, and A. L'Huillier, "Influence of atomic density in high-order harmonic generation," J. Opt. Soc. Am. B **13**(1), 148–156 (1996).
7. C. J. Lai and F. X. Kärtner, "The influence of plasma defocusing in high harmonic generation," Opt. Express **19**(23), 22377–22387 (2011).
8. D. M. Gaudiosi, B. Reagan, T. Popmintchev, M. Grisham, M. Berrill, O. Cohen, B. C. Walker, M. M. Murnane, H. C. Kapteyn, and J. J. Rocca, "High-Order Harmonic Generation from Ions in a Capillary Discharge," Phys. Rev. Lett. **96**(20), 203001 (2006).
9. B. A. Reagan, T. Popmintchev, M. E. Grisham, D. M. Gaudiosi, M. Berrill, O. Cohen, B. C. Walker, M. M. Murnane, J. J. Rocca, and H. C. Kapteyn, Enhanced high-order harmonic generation from Xe, Kr, and Ar in a capillary discharge," Phys. Rev. A **76**(1), 013816 (2007).
10. P. Arpin, T. Popmintchev, N. L. Wagner, A. L. Lytle, O. Cohen, H. C. Kapteyn, and M. M. Murnane, "Enhanced High Harmonic Generation from Multiply Ionized Argon above 500 eV through Laser Pulse Self-Compression," Phys. Rev. Lett. **103**(14), 143901 (2009).

#314618 https://doi.org/10.1364/OE.26.003067
Journal © 2017 Received 1 Dec 2017; revised 19 Jan 2018; accepted 21 Jan 2018; published 29 Jan 2018

Optics EXPRESS

11. F. Brizuela, C. M. Heyl, P. Rudawski, D. Kroon, L. Rading, J. M. Dahlström, J. Mauritsson, P. Johnsson, C. L. Arnold, and A. L'Huillier, "Efficient high-order harmonic generation boosted by below-threshold harmonics," Sci. Rep. **3**(1), 1410 (2013).
12. A. Rundquist, C. G. Durfee 3rd, Z. Chang, C. Herne, S. Backus, M. M. Murnane, and H. C. Kapteyn, "Phase-matched generation of coherent soft X-rays," Science **280**(5368), 1412–1415 (1998).
13. K. Cassou, S. Daboussi, O. Hort, O. Guilbaud, D. Descamps, S. Petit, E. Mével, E. Constant, and S. Kazamias, "Enhanced high harmonic generation driven by high-intensity laser in argon gas-filled hollow core waveguide," Opt. Lett. **39**(13), 3770–3773 (2014).
14. C. Jin, G. J. Stein, K. H. Hong, and C. D. Lin, "Generation of Bright, Spatially Coherent Soft X-Ray High Harmonics in a Hollow Waveguide Using Two-Color Synthesized Laser Pulses," Phys. Rev. Lett. **115**(4), 043901 (2015).
15. P. Wei, X. Yuan, C. Liu, Z. Zeng, Y. Zheng, J. Jiang, X. Ge, and R. Li, "Enhanced high-order harmonic generation from spatially prepared filamentation in argon," Opt. Express **23**(13), 17229–17236 (2015).
16. J. W. G. Tisch, T. Ditmire, D. J. Fraser, N. Hay, M. B. Mason, E. Springate, J. P. Marangos, and M. H. R. Hutchinson, "Investigation of high-harmonic generation from xenon atom clusters," J. Phys. B **30**(20), L709–L714 (1997).
17. C. Vozzi, M. Nisoli, J. P. Caumes, G. Sansone, S. Stagira, S. De Silvestri, M. Vecchiocattivi, D. Bassi, M. Pascolini, L. Poletto, P. Villoresi, and G. Tondello, "Cluster effects in high-order harmonics generated by ultrashort light pulses," Appl. Phys. Lett. **86**(11), 111121 (2015).
18. M. Aladi, R. Bolla, P. Rácz, and I. B. Földes, "Noble gas clusters and nanoplasmas in high harmonic generation," Nucl. Instrum. Methods Phys. Res. B **369**, 68–71 (2016).
19. T. D. Donnelly, T. Ditmire, K. Neuman, M. D. Perry, and R. W. Falcone, "High-Order Harmonic Generation in Atom Clusters," Phys. Rev. Lett. **76**(14), 2472–2475 (1996).
20. T. Ditmire, T. Donnelly, A. M. Rubenchik, R. W. Falcone, and M. D. Perry, "Interaction of intense laser pulses with atomic clusters," Phys. Rev. A **53**(5), 3379–3402 (1996).
21. M. Aladi, I. Márton, P. Rácz, P. Dombi, and I. B. Földes, "High harmonic generation and ionization effects in cluster targets," High Power Laser Sci. Eng. **2**, e32 (2014).
22. H. Park, Z. Wang, H. Xiong, S. B. Schoun, J. Xu, P. Agostini, and L. F. DiMauro, "Size-Dependent High-order Harmonic Generation in Rare-Gas Clusters," Phys. Rev. Lett. **113**(26), 263401 (2014).
23. Y. Tao, R. Hagmeijer, H. M. J. Bastiaens, S. J. Goh, P. J. M. Slot, S. G. Biedron, S. V. Milton, and K.-J. Boller, "Cluster size dependence of high-order harmonic generation," New J. Phys. **19**(8), 083017 (2017).
24. W. T. Mohamed, G. Chen, J. Kim, G. X. Tao, J. Ahn, and D. E. Kim, "Controlling the length of plasma waveguide up to 5 mm, produced by femtosecond laser pulses in atomic clustered gas," Opt. Express **19**(17), 15919–15928 (2011).
25. G. Chen, A. S. Boldarev, X. Geng, Y. Xu, Y. Cao, Y. Mi, X. Zhang, L. Wang, and D. E. Kim, "Investigation of the on-axis atom number density in the supersonic gas jet under high gas backing pressure by simulation," AIP Adv. **5**(10), 107220 (2015).
26. T. Ditmire, R. A. Smith, and M. H. R. Hutchinson, "Plasma waveguide formation in predissociated clustering gases," Opt. Lett. **23**(5), 322–324 (1998).
27. V. Kumarappan, K. Y. Kim, and H. M. Milchberg, "Guiding of intense laser pulses in plasma waveguides produced from efficient, femtosecond end-pumped heating of clustered gases," Phys. Rev. Lett. **94**(20), 205004 (2005).
28. G. Chen, X. Geng, T. W. Mohamed, H. Xu, Y. Mi, J. Kim, and D. E. Kim, "Ar plasma waveguide produced by a low-intensity femtosecond laser," Opt. Commun. **285**(10), 2627–2631 (2012).
29. S. P. Le Blanc and R. Sauerbrey, "Spectral, temporal, and spatial characteristics of plasma-induced spectral blue shifting and its application to femtosecond pulse measurement," J. Opt. Soc. Am. B **13**(1), 72–88 (1996).
30. O. F. Hagena, "Cluster ion sources," Rev. Sci. Instrum. **63**(4), 2374–2379 (1992).
31. G. Chen, B. Kim, B. Ahn, and D. E. Kim, "Pressure dependence of argon cluster size for different nozzle geometries," J. Appl. Phys. **106**(5), 053507 (2009).
32. T. Kita, T. Harada, N. Nakano, and H. Kuroda, "Mechanically ruled aberration-corrected concave gratings for a flat-field grazing-incidence spectrograph," Appl. Opt. **22**(4), 512–513 (1983).
33. H. R. Lange, A. Chiron, J. F. Ripoche, A. Mysyrowicz, P. Breger, and P. Agostini, "High-Order Harmonic Generation and Quasiphase Matching in Xenon Using Self-Guided Femtosecond Pulses," Phys. Rev. Lett. **81**(8), 1611–1613 (1998).
34. J. W. G. Tisch, "Phase-matched high-order harmonic generation in an ionized medium using a buffer gas of exploding atomic clusters," Phys. Rev. A **62**(4), 041802 (2000).
35. Y. Wang, Y. Liu, X. Yang, and Z. Xu, "Spectral splitting in high-order harmonic generation," Phys. Rev. A **62**(6), 063806 (2000).
36. D. S. Steingrube, T. Vockerodt, E. Schulz, U. Morgner, and M. Kovačev, "Phase matching of high-order harmonics in a semi-infinite gas cell," Phys. Rev. A **80**(4), 043819 (2009).
37. M. Lewenstein, P. Balcou, M. Y. Ivanov, A. L'Huillier, and P. B. Corkum, "Theory of high-harmonic generation by low-frequency laser fields," Phys. Rev. A **49**(3), 2117–2132 (1994).
38. M. V. Ammosov, N. B. Delone, and V. Krainov, "Tunnel ionization of complex atoms and of atomic ions in an alternating electric field," Sov. Phys. JETP **64**, 1191–1194 (1986).

Optics EXPRESS

39. E. Priori, G. Cerullo, M. Nisoli, S. Stagira, S. De Silvestri, P. Villoresi, L. Poletto, P. Ceccherini, C. Altucci, R. Bruzzese, and C. De Lisio, "Nonadiabatic three-dimensional model of high-order harmonic generation in the few-optical-cycle regime," Phys. Rev. A **61**(6), 063801 (2000).
40. http://henke.lbl.gov/optical_constants/
41. H. J. Shin, D. G. Lee, Y. H. Cha, J. H. Kim, K. H. Hong, and C. H. Nam, "Nonadiabatic blueshift of high-order harmonics from Ar and Ne atoms in an intense femtosecond laser field," Phys. Rev. A **63**(5), 053407 (2001).

1. Introduction

Generation of high-order harmonics (HHs) is a popular method to get coherent extreme ultraviolet (XUV) light, which has many applications in science and technology [1–4]. However, many applications require higher HH photon flux of HHs. However, the increase of laser intensity for a higher HH flux is limited by ionization-induced laser-defocusing in gas samples [5–7]. A waveguide configuration is one approach to overcome plasma-induced laser beam defocusing. By using a plasma waveguide preformed in gas-filled capillary discharges, the harmonic flux would be increased and the cutoff could be extended [8–10]. A dual-cell scheme can also increase the HH conversion efficiency [11].

Another approach is the quasi-phase-matching technique in a modulated and gas-filled hollow-core waveguide. This process increases HH output by a factor of 10^2 to 10^3 compared to that in non-phase-matched case [12]. Photon flux of HHs has also been increased by using a guided configuration at a laser intensity that greatly exceeds saturation intensity [13]. The enhanced harmonic yield has been obtained using synthesized two-color laser pulses and optimized waveguide configuration [14]. Spatially-prepared filamentation in Ar gas cell can intensify HH by nearly an order of magnitude [15].

Atomic clusters are more efficient than monatomic gas as sources of coherent ultraviolet light [16–19]. They absorb laser light efficiently, which results in heated electrons, rapid production of ions and x-ray emission [20]. The properties of an atomic cluster for HH have been investigated in detail [21]. The dependence of HH on cluster size was investigated [22, 23], in which the contributions from clusters and gas monomers was also investigated, showing that clusters are more efficient radiators. Hence the combination of a waveguiding technique and cluster target should further increase HH photon flux.

In this letter, we demonstrate the enhancement of HHs in a plasma waveguide configuration formed in a clustered Ar gas. A gas jet with a slit nozzle is used to generate Ar clusters [24, 25] at a backing pressure of 10 bars. We demonstrate guiding in an end-pumped waveguide generated in a clustered gas [26–28]. Plasma waveguide formation using a pre-pulse is investigated by analyzing time-resolved interferograms from a Michelson interferometer (MI). The electron density of a waveguide is extracted from the interferogram by Abel inversion. By the interaction of another delayed femtosecond laser pulse with the plasma waveguide, the HH is generated and enhanced by a factor of nine at the 27th-order harmonic, compared to the case without a waveguide. Numerical simulation by solving the time-dependent Schrödinger equation in strong field approximation showed the enhancement and the blue shift of HHs that agree well with experiment results. This result shows that the blue shift of HH is caused by a blue shift of the fundamental laser frequency as a consequence of self-phase modulation (SPM) [29].

2. Experimental setup

The experiment [Fig. 1] used a 10-Hz chirped pulse amplification (CPA) laser at 790 nm with a pulse duration of 35 fs FWHM and a pulse energy of 35 mJ. The beam was split in a 2:3 ratio into a low-energy pulse (P1) and a high-energy pulse (P2) by a beam splitter. P1 is a pre-pulse that is used to create a plasma waveguide in a clustered Ar gas. P2 is a drive pulse, which is delayed. P1 and P2 were combined by a beam combiner, then focused on a clustered Ar gas by a lens (L) with a focal length of 50 cm. The beam radius at focus was about 125 μm. Clusters are formed by a supersonic slit nozzle (0.5 mm × 5 mm) [Fig. 1 inset] installed above the pulsed valve (Parker series 99 with 0.5 mm diameter orifice). The nozzle and gas

Optics EXPRESS

jet can be precisely positioned by a motorized X-Y-Z stage to a laser focus in vacuum. The average cluster size was about several nanometers under Ar gas backing pressure of 10 bar [30]. Each cluster had a

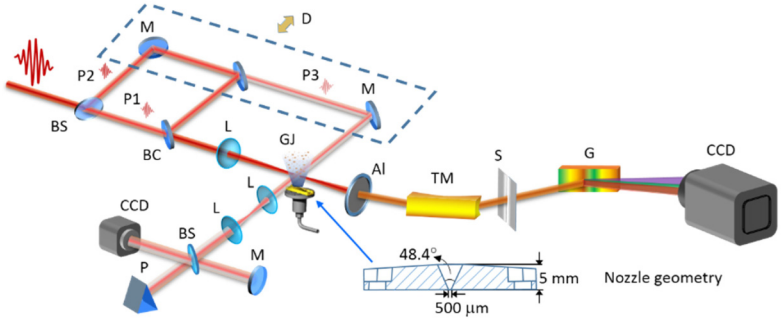

Fig. 1. Experimental setup (BS: beam splitter, M: mirror, D: delay line, L: lens, BC: beam combiner, P: prism, GJ: gas jet, Al: Aluminum filter, TM: toroidal mirror, S: slit, G: grating, P1: pre-pulse, P2: drive pulse, P3: transverse probe pulse). Inset: geometry of nozzle.

radius of ~1.7 nm, (composed of an average of ~450 atoms), as estimated using Rayleigh scattering [31]. The gas jet was synchronized by a DG535 (Stanford Research System) with the pre-pulse. The calculated peak intensities were 3.0×10^{14} W/cm^2 for P1 and 4.5×10^{14} W/cm^2 for P2. The leakage light (P3) from the delay-line mirror was used to probe the waveguide by using a Michelson Interferometer (MI). Two lenses were used to image the plasma waveguide on a CCD in the MI. The interferogram encodes the information of the phase shift due to a cylindrically symmetric plasma. By varying the probe time with respect to P1, the evolution of the laser plasma waveguide was investigated. To get the HH spectrum, HHs were collected and focused by a toroidal mirror onto the slit of a flat-field XUV spectrometer [32], and the infrared light was blocked by a 0.8-µm-thick Al film.

3. Results and discussions

3.1 Experiment

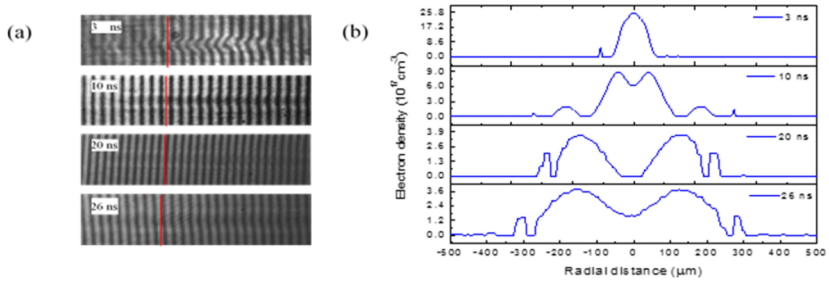

Fig. 2. (a): Interferometric images of Ar waveguide by the pre-pulse at different probe times; (b): De-convoluted electron density profiles of the waveguides at marked red lines in (a).

We investigated the waveguide formation by P1 without P2, by using a transverse P3 at different time delays t_D, to optimize the time for waveguide formation. Interferograms [Fig. 2(a)] of the Ar plasma waveguide created by P1 were captured at $3 \leq t_D \leq 26$ ns. The electron densities [Fig. 2(b)] of the waveguide were extracted from the interferogram by Abel inversion

Optics EXPRESS

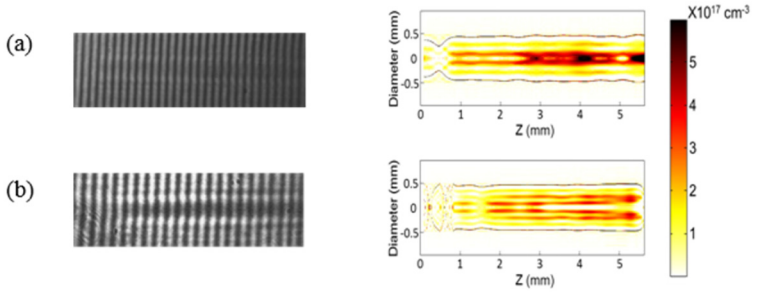

Fig. 3. Plasma waveguide (a) without a drive pulse (b) with a drive pulse at 20 ns delay time.

at the red lines in Fig. 2(a). Without P2, a good waveguide was formed ~20 ns after the interaction of P1 with the clustered gas. At t_D = 20 ns, the profile [Fig. 3(a)] of the plasma waveguide from P1 was not completely open along the propagation direction [Fig. 3(a)]. The Injection of P2 into the waveguide at t_D = 20 ns opened it completely [Fig. 3(b)].

The beam profiles of the drive pulse P2 passing through the waveguide for different delays are shown in Fig. 4. The intensity of the output beam was weak before the waveguide was formed. The reason is that the drive pulse is absorbed and refracted out when a waveguide is not properly formed; the beam gets stronger as waveguide is being formed. The highest throughput of 70% was achieved at t_D = 20 ns. The beam profile and strong intensity of P2 confirms that the pulse propagated through the waveguide. In subsequent measurements we used t_D = 20 ns to guide P2.

To distinguish the contribution of P1 to HH intensity, the spectra [Fig. 5] were measured for three cases: (1) P1 only, (2) P2 without a waveguide and (3) P2 with a waveguide; 1500 shots were accumulated for each spectrum. When only P1 was used, the channel is not completely open along the propagation direction, as seen in Fig. 3(a). The electron density of the 2nd half of the channel is in the order of a few x $10x^{17}cm^{-3}$. Ar density is then expected to be in the order of 10^{18} cm^{-3}. The transmission in the spectral region of our interest is negligibly small. In case of P2 with a higher intensity, a waveguide seems to be open all the way to the end. In this case. The phase matching conditions are better met with longer and more uniform wave guide [33]. The use of P2 with a waveguide clearly intensified HH whose order ≥ 19, *compared to the intensity of HH without a waveguide.*

Phase matching condition was met for a longer distance with a waveguide than without one. With a uniform waveguide [Fig. 3 (b)], the electric field of the HHs can be added together in phase in different parts of the waveguide, therefore the intensity of HH dispersive medium grows with the medium length. The enhancement was different at different orders because phase-matching conditions differ among orders due to electron dispersion [34]. The highest enhancement by a factor of nine occurred in the 27th-order harmonic. The HH frequency also shifted toward blue, as also reported in [21]. The HH spectrum split and broadened [Fig. 5(a)]; these effects occur when the driven laser intensity exceeds the ionization threshold (saturation intensity) of an Ar cluster. They are attributed to propagation effects in a rapidly ionizing medium [35], and to temporally-changing phase-matching conditions (transient phase matching) [36].

Optics EXPRESS

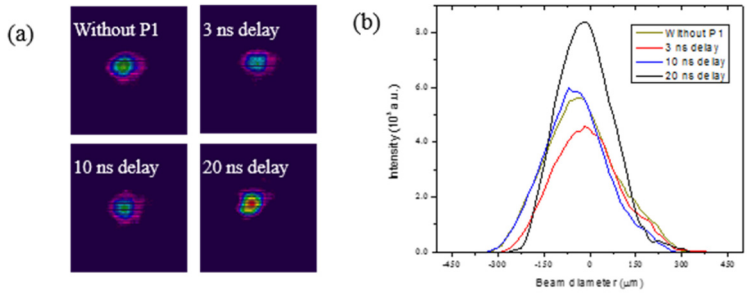

Fig. 4. (a) Beam profiles and (b) intensity distribution of the drive pulse for different delay times; 3 ns delay (red), 10 ns delay (blue), 20 ns delay (black).The exposure time for all images are the same.

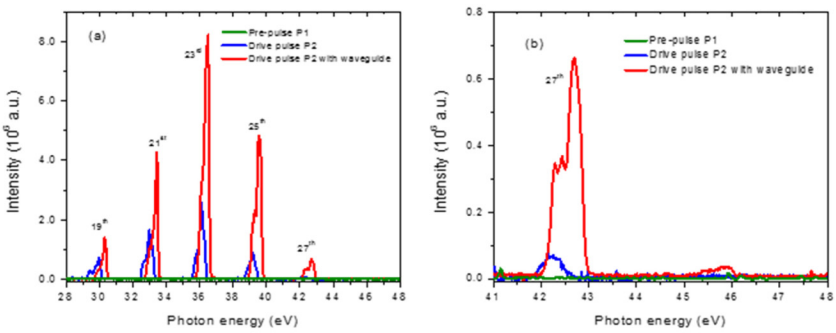

Fig. 5. (a) Experimental HH spectrum; (b) Experimental HH spectrum in the 41-48 eV spectral region: pre-pulse P1 (green), drive pulse P2 with (red) and without (blue) waveguide.

3.2 Numerical simulation

A single-atom response was simulated by solving the time-dependent Schrödinger equation in strong-field approximation [37]. HH is treated as the dipole radiation of an atom excited by the external laser field. We estimate d_{NL}, the expectation value of the dipole moment of an atom in time domain, which is $d_{NL}(\mathrm{t}) = \langle \Psi(\vec{r},t)|\vec{r}|\Psi(\vec{r},t)\rangle$, where $\Psi(\vec{r},t)$ is the time dependent wave function of the system. d_{NL} is then calculated as

$$d_{NL}(t) = 2\,\mathrm{Re}\{i\int_{-\infty}^{t} dt'(\pi/(\varepsilon + \frac{i(t-t')}{2}))^{3/2} a^*(t) d^*[p_s(t',t) - A(t')] \times \exp[-iS(t',t)]a(t)d[p_s(t',t) - A(t')]E_1(t')\}\exp[-\int_{-\infty}^{t} w(t')dt'] \quad (1)$$

where $E_1(t)$ is the electric field of an external laser, $A(t)$ the corresponding vector potential, d the bound-continuum transition element matrix, P_s and S are respectively the saddle point stationary of canonical momentum and quasi-classical action, and $a(t)$ is the amplitude of the ground state wave function which is calculated in the ADK model [38] The last term considers the ground-state depletion. The harmonic spectrum of the single-atom response is obtained by the Fourier transform of the dipole acceleration.

The macroscopic propagations of both the fundamental and the HH beam in a plasma waveguide are included by solving the non-adiabatic three-dimensional coupled wave equations [39]. The propagation of the fundamental beam in a plasma waveguide can be described in a moving coordinate frame by

Optics EXPRESS

$$\nabla_{\perp}^{2}\tilde{E}_{1}(r,z,\omega)-\frac{2i\omega}{c}[\frac{\partial\tilde{E}_{1}(r,z,\omega)}{\partial z}]=FT[\frac{\omega_{p}^{2}(r,z,t)}{c^{2}}E_{1}(r,z,t)], \quad (2)$$

where $\omega_p=(e^2n_e(r,z,t)/\varepsilon_0 m_e)^{1/2}$ is the plasma frequency and n_e the free-electron density. FT means Fourier transform and $\tilde{E}_1(r,z,\omega)$ is the Fourier transform of $E_1(r,z,t)$. The generation and propagation of HH are given by

$$\begin{aligned}&\nabla_{\perp}^{2}\tilde{E}_{h}(r,z,\omega)-\frac{2i\omega}{c}[\frac{\partial\tilde{E}_{h}(r,z,\omega)}{\partial z}+\frac{\alpha}{2}\tilde{E}_{h}(r,z,\omega)]\\&=FT[\frac{\omega_{p}^{2}(r,z,\omega)}{c^{2}}E_{h}(r,z,t)]-\omega^{2}\mu_{0}\tilde{P}_{NL}(r,z,\omega)\end{aligned} \quad (3)$$

where α is the XUV absorption coefficient in Ar obtained from [40], and $P_{NL}(r,z,t)=[n_0-n_e(r,z,t)]d_{NL}(r,z,t)$ is the nonlinear polarization. The dependence of α on the frequency is taken into account in the simulation. The single-atom response is inserted into the propagation equation as a source term. The plasma effect on the fundamental beam and the absorption of HH by the gas medium are also considered. The simulation was performed for the waveguide structure obtained experimentally at t_D = 20 ns [Fig. 3(b)]; the gradual decrease of the electron density along the propagation direction is also considered. The HH spectrum is integrated over space at the exit of the waveguide.

The numerical result [Fig. 6] was done for a fundamental beam with 35-fs FWHM at 790 nm with a peak intensity of 1.1 × 10^{14} W/cm^2 at the entrance of the waveguide, a beam waist of 140 μm (full width at $1/e^2$), and a propagation length of 10 mm. The difference between the simulation parameters and the experimental parameters may come from both uncertainties in experimental measurements and the simplification in simulation. Especially, the discrepancy in the medium length may represent the effect by clusters in the medium because the simulation is done with atomic argon, not including any effect from clusters. The calculation also showed enhancement of the 19th or higher-order harmonics, as observed in the experiment. The enhancement of HH is due to both the plasma waveguide in which the intense laser pulse can maintain a long propagation without defocusing and the phase-match condition met better for a longer distance than without the waveguide. The dipole phase (which is a function of the laser intensity) and the laser geometrical phase is maintained a longer distance by using the plasma channel. The simulation suggested that the blue shift of HH is due to a blue shift of the fundamental laser frequency. The fundamental beam frequency at a fixed beam size of 140 μm was blue-shifted as an electron density increased [Fig. 7]. The temporal change of electron

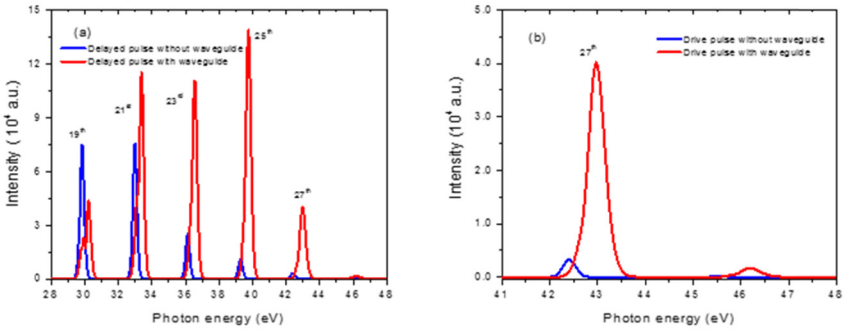

Fig. 6. (a) Simulated HH spectrum for drive pulse; (b) Simulated HH spectrum in the 41-48 eV spectral region: with (red) and without (blue) waveguide.

Optics EXPRESS

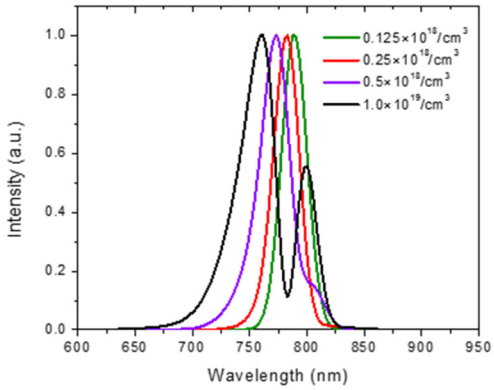

Fig. 7. The dependence of the blue shift of the fundamental wavelength of drive laser on electron density at a fixed beam waist of 140 μ m. Simulations are done with 35 fs FWHM at 790 nm and a peak intensity of 1.1×10^{14} W/cm^2.

density like the plasma channel causes the variation of the refractive index which introduces self-phase modulation (SPM). The frequency shift due to the SPM in an ionizing gas is proportional to the gas density [29], and yields the blue shift of high-order harmonics [41]. The splitting at the density of 1x 10^{19} cm^{-3} shown in Fig. 7 is estimated to be ~8.6x10^{-3} eV. This splitting would lead to the splitting of 0.2 eV for the 25th harmonic, which is still ~2x smaller than the experimental observation shown in Fig. 5. Hence the splitting in HH has a different origin. Further investigation will be carried out.

4. Conclusion

Appropriate formation of a waveguide in clustered Ar gas is demonstrated. Beam profiles emerging from a waveguide with different delays demonstrate that the throughput of the drive pulse increases as waveguide is being formed. HH was intensified by the plasma waveguide in which the intense laser pulse can make a longer propagation without defocusing in the waveguide, and because the phase matching conditions are better met than in the case without the waveguide. HH was intensified by a factor of nine at the 27th-order harmonic. Numerical simulation of HH generation in a plasma waveguide agreed well with experimental observation of the enhancement and blue shift of HH. The blue shift of HH is due to the blue shift of the fundamental laser frequency induced by SPM which resulted from the temporal change of electron density. This method is a simple way to intensify HH for applications that need high HH photon flux.

5. Funding

This research was supported in part by Global Research Laboratory Program [Grant No 2009-00439] and by Max Planck POSTECH/KOREA Research Initiative Program [Grant No 2016K1A4A4A01922028] through the National Research Foundation of Korea (NRF) funded by the Ministry of Science and ICT, and the International Joint Research Program of National Natural Science Foundation of China [Grant No: 61210017].